



TITLE:

<Advanced Research Center for Beam Science>Electron Microscopy and Crystal Chemistry

AUTHOR(S):

CITATION:

<Advanced Research Center for Beam Science>Electron Microscopy and Crystal Chemistry. ICR Annual Report 2019, 26: 46-47

ISSUE DATE:

2019

URL:

<http://hdl.handle.net/2433/250268>

RIGHT:

Copyright © 2020 Institute for Chemical Research, Kyoto University

Advanced Research Center for Beam Science – Electron Microscopy and Crystal Chemistry –

<http://eels.kuicr.kyoto-u.ac.jp/Root/English>



Prof
KURATA, Hiroki
(D Sc)



Assoc Prof
HARUTA, Mitsutaka
(D Sc)



Assist Prof
NEMOTO, Takashi
(D Sc)



Program-Specific Res*
OGAWA, Tetsuya
(D Sc)



Program-Specific Res*
KIYOMURA, Tsutomu

*Nanotechnology Platform

Researcher (pt)

YAMAGUCHI, Atsushi

Students

LAI, Ming Wei (D3)

SHINYA, Tomoki (M2)

TOBA, Tomohito (M2)

IWASHIMIZU, Chisaki (M2)

KAWAGUCHI, Tomoki (M1)

Scope of Research

We study crystallographic and electronic structures of materials and their transformations through direct imaging of atoms or molecules by high-resolution electron spectromicroscopy, which realizes energy-filtered imaging and electron energy-loss spectroscopy as well as high-resolution imaging. By combining this with scanning probe microscopy, we cover the following subjects: 1) direct structure analysis, electron crystallographic analysis, 2) elemental analysis and electronic states analysis, 3) structure formation in solutions, and 4) epitaxial growth of molecules.



KEYWORDS

STEM-EELS

Spectrum Imaging

Extremely Low Count Detection

Gain Normalized Spectrum

Read-out Noise

Selected Publications

Saito, H.; Kurata, H., Formation of a Hybrid Plasmonic Waveguide Mode Probed by Dispersion Measurement, *J. Appl. Phys.*, **117**, [133107-1]-[133107-7] (2015).

Haruta, M.; Hosaka, Y.; Ichikawa, N.; Saito, T.; Shimakawa, Y.; Kurata, H., Determination of Elemental Ratio in an Atomic Column by Electron Energy-Loss Spectroscopy, *ACS Nano*, **10**, 6680-6684 (2016).

Haruta, M.; Fujiyoshi, Y.; Nemoto, T.; Ishizuka, A.; Ishizuka, K.; Kurata, H., Atomic-Resolution Two-Dimensional Mapping of Holes in the Cuprate Superconductor $\text{La}_{2-x}\text{Sr}_x\text{CuO}_{4+\delta}$, *Phys. Rev. B*, **97**, [205139-1]-[205139-5] (2018).

Yamaguchi, A.; Haruta, M.; Nemoto, T.; Kurata, H., Probing Directionality of Local Electronic Structure by Momentum-Selected STEM-EELS, *Appl. Phys. Lett.*, **113**, [053101-1]-[053101-4] (2018).

Haruta, M.; Fujiyoshi, Y.; Nemoto, T.; Ishizuka, A.; Ishizuka, K.; Kurata, H., Extremely Low Count Detection for EELS Spectrum Imaging by Reducing CCD Read-out Noise, *Ultramicroscopy*, **207**, [112827-1]-[112827-6] (2019).

Extremely Low Count Detection for EELS Spectrum Imaging by Reducing CCD Read-out Noise

Electron energy-loss spectroscopy (EELS) combined with scanning transmission electron microscopy (STEM) is useful for examining local chemical elements, electronic structure, and optical excitation with high spatial resolution. However, it is not easy to obtain high signal-to-noise ratio (SNR) spectra with high spatial resolution without sample damage. Summation of many spectra obtained by multiple spectrum imaging (SI) measurement with low dose rate is often used to prevent the sample damage. In the present contribution, we report a systematic statistical study on the reduction of CCD noise for EELS using our original method.

STEM-EELS experiments were carried out on a JEM-ARM200F (200 kV, JEOL) using a GIF Quantum ERS (Gatan) for EELS acquisition and Gatan Microscopy Suite (GMS, Gatan) for the analysis. 2048×260 2D CCD signals are binned by hardware/software along y direction to produce 2048 channel 1D EELS spectrum.

In general, an EELS spectrum is acquired in the gain normalized mode. In this mode, the obtained spectrum I_G is described as

$$I_G = \sum_y ([S_{x,y} + D_{x,y}] - D_{x,y}^s) G_{x,y},$$

where $S_{x,y}$ is an EELS signal derived from incident electrons, $D_{x,y}$ is dark reference, $D_{x,y}^s$ is a single frame dark reference measured with beam blanking and $G_{x,y}$ is a gain correction, which is saved as the reciprocal of the gain reference image measured with the uniform radiation condition in the TEM mode. $[]$ indicates integer processing by analog-to-digital conversion. The main component of the dark reference is read-out offset and read-out noise. Unfortunately, this common process inevitably gives rise to fixed pattern noise derived from the difference between the average of the dark reference $[D_{x,y}]$ and $D_{x,y}^s$. To remove such fixed pattern noise, recent GMS software has added a HQ (high-quality) dark reference option in post-processing. The HQ spectrum HQI_G is

$$HQI_G = \{I_G + \sum_y (D_{x,y}^s G_{x,y})\} - \sum_y (\langle [D_{x,y}] \rangle G_{x,y}),$$

where $\langle [D_{x,y}] \rangle$ is the average dark reference image. However HQI_G cannot completely remove the above noise due to the integer process. As an alternative, we obtain the ultra-high-quality (UHQ) dark subtracted spectrum $UHQI_D$ by subtracting the UHQ dark reference $UHQD_U = \sum_y [D_{x,y}]$ from the experimental spectra I_U in the unprocessed mode without the integer process:

$$UHQI_D = I_U - UHQD_U = \sum_y [S_{x,y} + D_{x,y}] - \sum_y [D_{x,y}].$$

In this case, if $UHQD_U$ is the population mean of the dark reference, the noise derived from the dark reference

could be suppressed by the summation. The UHQ gain normalized spectrum $UHQI_G$ is obtained by using the average gain reference data generated by averaging the vertical 260 channels of the gain correction image:

$$UHQI_G = UHQI_D \times \sum_y G_{x,y}.$$

A histogram of the intensity of the dark read-out at a single channel is close to a Gaussian distribution. This means that if the population mean of the dark read-out at individual channels was subtracted, the noise could be suppressed by a summation over many measurements. The noise standard deviation of the dark read-out over 2048 spectral channels after subtraction of $UHQD_U$ (using n_a frames) as a function of the accumulation number n_s become much less than one count above $n_s = 5000$ for $n_a \geq 5000$. Therefore, it may be possible to visualize even a single signal count per spectrum by summation of the spectrum, if we use a good averaged dark reference.

As a test experiment, the Ti $L_{2,3}$ -edge was measured from SrTiO₃. $UHQD_U$ was estimated using 20,000 spectra. Figure 1(a) shows a single frame Ti $L_{2,3}$ -edge spectrum of $UHQI_G$ in the SI data obtained with a very low dose. Figure 1(b) shows 12,000-frame summed spectra after different spectral treatments. The average peak intensity of the first peak was about 1.2 counts, which corresponds to 0.15 electrons per dwell time. This is a demonstration of the detection of a single inelastic electron per channel in a spectrum during the dwell time. The result of gain averaging by shifting the spectrum over 200 channels after $UHQI_G$ shows a further improvement of the noise standard deviation (0.092 counts), and this process is very effective. A combination of the subtraction of the $UHQD_U$ and the gain averaging is the best method. Even a single-electron core-loss signal per spectrum can be visualized as a high-SNR spectrum using the present technique.

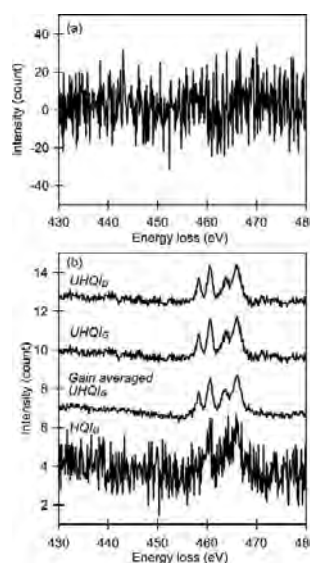


Figure 1. (a) A single-frame $UHQI_G$ of the Ti $L_{2,3}$ -edge spectrum of SrTiO₃ extracted from SI data obtained with a very weak signal. (b) Spectra averaged over 12,000 frames after different spectral treatments. The spectral intensities were normalized as a single spectrum. Each spectrum is vertically shifted by 3 counts except for the bottom spectrum (HQI_G).